Acta Crystallographica Section B
Structural Science
ISSN 0108-7681

Amino and cyano N atoms in competitive situations: which is the best hydrogen-bond acceptor? A crystallographic database investigation

Nahossé Ziao, Jérôme Graton, Christian Laurence and Jean-Yves Le Questel*

Laboratoire de Spectrochimie, Faculté des Sciences et des Techniques de Nantes, 2 rue de la Houssinière, BP 92208 44322 Nantes CEDEX 3, France

Correspondence e-mail:
jean-yves.lequestel@chimie.univ-nantes.fr

Received 20 June 2001
Accepted 19 September 2001

The relative hydrogen-bond acceptor abilities of amino and cyano N atoms have been investigated using data retrieved from the Cambridge Structural Database and *via ab initio* molecular orbital calculations. Surveys of the CSD for hydrogen bonds between HX (X = N, O) donors, N—T—C≡N (push–pull nitriles) and N—(Csp^3)$_n$—C≡N molecular fragments show that the hydrogen bonds are more abundant on the nitrile than on the amino nitrogen. In the push–pull family, in which T is a transmitter of resonance effects, the hydrogen-bonding ability of the cyano nitrogen is increased by conjugative interactions between the lone pair of the amino substituent and the C≡N group: a clear example of resonance-assisted hydrogen bonding. The strength of the hydrogen-bonds on the cyano nitrogen in this family follows the experimental order of hydrogen-bond basicity, as observed in solution through the p$K_{\rm HB}$ scale. The number of hydrogen bonds established on the amino nitrogen is greater for aliphatic aminonitriles N—(Csp^3)$_n$—C≡N, but remains low. This behaviour reflects the greater sensitivity of the amino nitrogen to steric hindrance and the electron-withdrawing inductive effect compared with the cyano nitrogen. *Ab initio* molecular orbital calculations (B3LYP/6-31+G** level) of electrostatic potentials on the molecular surface around each nitrogen confirm the experimental observations.

© 2001 International Union of Crystallography
Printed in Great Britain – all rights reserved

1. Introduction

Hydrogen bonding is one of the most important intermolecular interactions involved in supramolecular chemistry, particularly in protein–ligand interactions (Jeffrey & Saenger, 1991) and crystal engineering (Desiraju, 1997; Aakeröy, 1997). An attractive way to study intermolecular hydrogen bonding is offered by the Cambridge Structural Database (CSD; Allen *et al.*, 1991). Since a crystal is the ultimate supermolecule, the CSD contains a plethora of information relevant to intermolecular interactions in general. The CSD has been the basis for extensive statistical studies on the properties of various hydrogen-bond (HB) acceptors, *e.g.* Nsp^2 (Llamas-Saiz & Foces-Foces, 1992), carbonyl, ether and ester O atoms (Lommerse *et al.*, 1997), sulfur in C=S systems (Allen, Baalham *et al.*, 1997), nitro- (Allen, Bird *et al.*, 1997) and nitrile groups (Le Questel *et al.*, 2000; Thallapally & Desiraju, 2000). A database of experimental and theoretical information on non-bonded interactions for a wide range of functional groups is offered by the program *ISOSTAR* (Bruno *et al.*, 1997), part of the distributed CSD system since 1997. However, CSD studies devoted to the relative HB abilities of various functional groups in competitive situations are scarce. Etter & Reutzel (1991) first tried to rank the relative proton accepting abilities of several organic functions by analyzing their molecular packing in crystalline systems. These studies showed that hydrogen-bond accepting properties of functional groups clearly depend on their local intramolecular environment. Recently, Böhm *et al.* (1996) and Nobeli *et al.* (1997) used statistical analyses of intermolecular interactions in the crystal structures of organic molecules to investigate the hydrogen-bonding behaviour of O and N atoms in competitive situations. Such studies not only provide structural features about the HB interactions of the various functional groups selected, but also guidelines for a chemical rationale of the HB selectivity properties observed.

In our group, the strength of hydrogen-bond acceptors (HBA) is measured from the Gibbs energy change $\Delta G_{\rm HB}$ for the formation of 1:1 hydrogen-bonding complexes between HBA and a reference HB donor (4-fluorophenol) in tetrachloromethane at 298 K [equations (1)–(3)]. The p$K_{\rm HB}$ database (5.707 p$K_{\rm HB} = -\Delta G_{\rm HB}$ kJ mol^{-1})

$$\mathrm{B} + 4\text{-}\mathrm{FC_6H_4OH} \rightleftharpoons 4\text{-}\mathrm{FC_6H_4OH}\cdots\mathrm{B} \qquad (1)$$

$$K\ (\mathrm{dm^3\ mol^{-1}}) = [\mathrm{Complex}]/[\mathrm{Base}][4\text{-}\mathrm{FC_6H_4OH}] \qquad (2)$$

$$\mathrm{p}K_{\rm HB} = \log K = (\Delta G^0\ \mathrm{kJ\ mol^{-1}})/5.71 \qquad (3)$$

comprises today *ca* 1000 HBA and has been extended, since the pioneering work of Taft's group (Gurka & Taft, 1969; Taft *et al.* 1969), to various families of organic bases such as nitrogen (Graton *et al.*, 1999), oxygen (Le Questel *et al.*, 1992; Besseau *et al.*, 1994; Chardin *et al.*, 1996*a*,*b*), sulfur (Laurence *et al.*, 1995) and carbon bases (Besseau *et al.*, 1996). In 'push–pull' systems, R_2NA or R_2NTA, the nitrogen lone-pair delocalization towards the resonance acceptor group (*e.g.* NO$_2$ or C≡N), either directly or through a transmitter group *T* (*e.g.* vinylogous amides), becomes so significant that the nitrogen loses its HB ability to the benefit of the pulling *A* group. Furthermore, the *A* group becomes super-basic in hydrogen bonding (Laurence & Berthelot, 2000). In R_2N—C≡N (I) and R_2N—*T*—C≡N (II*a*)–(*c*) systems the competition between amino and cyano N atoms, and the relation between the nature of the transmitter group *T* and the relative order of the nitrile nitrogen HB basicity is well characterized on the p$K_{\rm HB}$ scale (Berthelot, Helbert, Laurence, Le Questel, Anvia & Taft, 1993). When the functional group separating the amino and nitrile N atoms is saturated: [C(sp^3)$_n$ (III)], the interruption of the transmission of conjugative interactions between the two organic functions makes the amino nitrogen a good candidate for HB interactions. Our FTIR measurements in dilute solution on these systems confirm unambiguously the formation of two 1:1 hydrogen-bonded complexes on amino and cyano N atoms, respectively (Graton *et al.*, 2001), the contribution of the amino nitrogen atom increasing with the lengthening of the saturated chain.

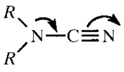

(I)

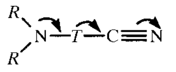

T = (II*a*) Ph
(II*b*) CH═CH
(II*c*) CH═N

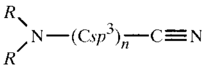

(III)
n = 1, 2, 3 and 4

(I), (II*a*–*c*), (III) *R* = H, Csp^3

In the present work we have used the CSD to investigate the hydrogen-bonding competition between amino and cyano N atoms in R_2N—C≡N, R_2N—*T*—C≡N and R_2N—(Csp^3)$_n$—C≡N systems as a function of the group separating the two N atoms. The hydrogen-bonding properties of nitrogen in isocyanides (Alkorta *et al.*, 1998) and nitriles (Le Questel *et al.*, 2000; Thallapally & Desiraju, 2000) have recently been the subject of CSD statistical analyses but, to our knowledge, no systematic investigation devoted to the hydrogen-bonding competition between cyano N atoms and other HBA has been published. To address this problem we have focused on several issues. First, the analysis of relevant geometric parameters of both types of N atoms for systems (I), (II*a*)–(*c*) and (III) has allowed the characterization of the structural features of 'push–pull' nitriles and aliphatic nitriles. Secondly, the occurrence of hydrogen-bonding interactions on both HBA in systems (I), (II*a*)–(*c*) and (III) is reported and their geometrical characteristics analysed. The strength of the HB interactions established on the nitrile nitrogen, followed by the HB lengths, have then been compared with the experimental order of HB basicity observed on the p$K_{\rm HB}$ scale for comparable systems. Finally, *ab initio* calculations of molecular electrostatic potentials at the B3LYP/6–31+G** level have been undertaken on models of the various molecular fragments investigated. The evolution of the values computed around each nitrogen has been related to the experimental order of HB basicity observed in solution through the p$K_{\rm HB}$ scale and to the crystallographic data. We also show that the angular locations of the electrostatic potential surface minima agree well with the directionality of the HB interactions observed in the solid state.

2. Methodology

2.1. Database searches

All crystallographic data were retrieved from the October 1999 (197 481 entries) release of the Cambridge Structural Database (Allen *et al.*, 1991). Searches for bonded substructures and intermolecular non-bonded contacts in R_2N—C≡N, R_2N—*T*—C≡N and R_2N—(Csp^3)$_n$—C≡N systems were carried out using the program *QUEST3D* (Cambridge Structural Database, 1994). Subsequent data analyses were performed with *VISTA* (Cambridge Structural Database, 1995).

Substructures were only located in entries that

(i) are organic compounds within CSD chemical class definitions,

(ii) have error-free coordinate sets in CSD check procedures,

(iii) exhibit no crystallographic disorder,

(iv) contain no polymeric connections and

(v) have a crystallographic R factor $\leq$ 0.10.

All H atoms involved in non-bonded contact searches were placed in normalized positions, *i.e.* they were repositioned along their X-ray determined X—H vectors at a distance from O or N equal to the appropriate mean bond length established from neutron studies (Allen *et al.*, 1987).

The various fragments searched, together with their respective geometric parameters, are shown in Fig. 1 using the example of push–pull nitriles. The C≡N bond lengths d(C≡N), the valence angles around the amino nitrogen (τ_1, τ_2 and τ_3), and the displacement (h) of the amino nitrogen relative to the plane defined by its three substituents, were collected for each entry in which both amino and nitrile N atoms were *not involved in hydrogen-bond interactions*, since these interactions have an influence on the molecular geometry. In order to avoid competitive conjugative interactions the two remaining substituents on the amino nitrogen were restricted to H or Csp^3 atoms.

Non-bonded contact searches and geometrical analyses of interactions involving HX (X = N, O) hydrogen-bond donors and Nsp/Nsp^3 acceptors in systems (I), (II*a*)–(*c*) and (III) were carried out using the parameters indicated in Figs. 2(*a*) and (*b*), respectively: d(C≡N), the nitrile bond length, the N···H HB distances and the HB angles θ_1(C≡N···H), θ_2(Csp^3Nsp^3···H) and α_1(Nsp···H—X), α_2(Nsp^3···H—X). The α values relate to the directionality at donor-H, while the θ values relate to hydrogen-bond directionality at the acceptor atom. For all contact searches, the length of the hydrogen bond was accepted using as the upper limit the sum of the van der Waals radii of the hydrogen and the nitrogen acceptor atoms: 2.65 Å, with 1.55 Å for N and 1.10 Å for H (Rowland & Taylor, 1996). The other constraint required that $90 \leq \alpha_1, \alpha_2 \leq 180°$.

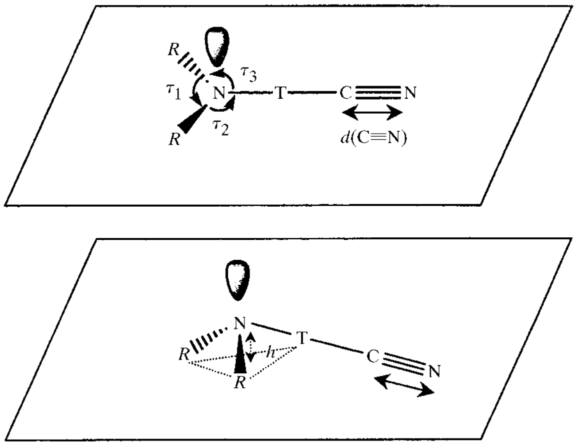

Figure 1
Definition of the geometrical parameters describing the structural features of the amino and nitrile moieties in the molecular fragments searched in the CSD.

Table 1
Observed geometries of amino and nitrile moieties in systems (I), (II*a*)–(*c*) and (III).

The data refer to structures in which the two HB acceptors are not involved in HB interactions. $N_{\rm ent}$ is the number of refcodes; $N_{\rm obs}$ is the number of observations (number of fragments in the refcodes). τ corresponds to the mean of the three valence angles around the amino N atom.

System	$N_{\rm ent}$ $N_{\rm obs}$	d(C≡N)	τ (°)	h (Å)
(I)	11 (14)	1.140 (7)	118 (1)	0.19 (2)
(II*a*)	12 (16)	1.146 (1)	117.7 (5)	0.19 (3)
(II*b*)	47 (68)	1.148 (2)	118.7 (4)	0.10 (2)
(II*c*)	9 (12)	1.153 (3)	119.8 (1)	0.05 (1)
(III)†	124 (154)	1.135 (1)	112.0 (4)	0.40 (1)

† For n = 1, 2, 3 and 4 (see text).

2.2. *Ab initio* calculations

Ab initio molecular orbital calculations for model compounds were carried out with the programs *Spartan*4.0 (Wavefunction, Inc., 1995) and *Gaussian*94 (Frisch *et al.*, 1995). The electrostatic potentials were computed at the B3LYP/6-31+G** level on fully optimized geometries. These surfaces were mapped onto the electron density surfaces (0.001 e bohr^{-3} isocontour) at high resolution. The angular locations of the various minima were calculated on the grid generated for these surfaces using the *Molden* program (Schaftenaar & Noordik, 2000).

3. Results and discussion

3.1. Cambridge Structural Database studies

An obvious use of the CSD is to derive molecular dimensions of functional groups in a very wide range of chemical environments. In this part, we will therefore first use the CSD to derive standard values for the nitrile and amino moieties of systems (I), (II*a*)–(*c*) and (III). Secondly, the CSD will be used to analyse the geometrical characteristics of the intermolecular hydrogen bonds formed on the amino and cyano N atoms in these various systems.

3.1.1. Observed geometries. Table 1 shows the mean values of the various geometrical descriptors of the amino and nitrile moieties in systems (I), (II*a*)–(*c*) and (III). As mentioned in §2,

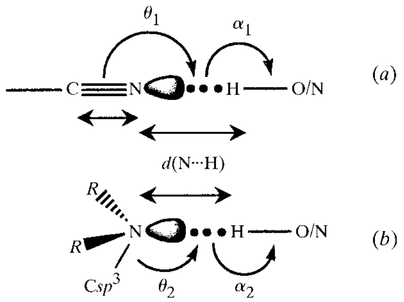

Figure 2
Definition of the geometrical parameters describing the hydrogen-bonding interactions on (*a*) the nitrile and (*b*) the amino N atoms of the various systems searched in the CSD.

these data refer to fragments not involved in HB interactions. The nitrile bonds are significantly lengthened in most of the push–pull systems [from 1.140 (1) (II*a*) to 1.153 (3) Å (II*c*)] compared with the values obtained for saturated nitriles [1.135 (1) Å (III)]. This behaviour is illustrated in Figs. 3(*a*) and (*b*), which show the histograms of the $d(\mathrm{C}\equiv\mathrm{N})$ bond lengths in systems (II*b*) and (III), respectively. The low number of cyanamides (I) does not allow the same conclusions to be drawn in the light of the estimated standard deviations (e.s.d.s) obtained [1.140 (7) Å]. The mean of the valence angles (τ_1, τ_2 and τ_3) around the amino nitrogen reveals another interesting structural feature: in push–pull systems this value is significantly greater: from 117.7 (5) (II*a*), 118 (1) (I) to 119.8 (1)° (II*c*), than in saturated aminonitriles [112.0 (4)°]. In systems (I) and (II*a*)–(*c*), these values are close to those of a trigonal nitrogen (120°), whereas in the third the mean of the τ angles tends to a value more characteristic of a tetrahedral nitrogen of sp^3 hybridization (107°). The analysis of the displacement of the amino nitrogen relative to the plane defined by its three substituents (h) confirms these features since it is significantly smaller in push–pull systems [from 0.05 (1) (II*c*) to 0.19 (3) Å (II*b*)] than in saturated aminonitriles [0.40 (1) Å]. On the whole, these structural parameters reflect the strong conjugative interactions between the amino lone pair and the nitrile nitrogen in push–pull nitriles compared with the saturated systems. Among the various groups able to transmit resonance effects between the 'pushing' $-\mathrm{N}R_2$ and the 'pulling' $-\mathrm{C}\equiv\mathrm{N}$ substituents studied in this work, the $\mathrm{C}=\mathrm{N}$ double bond behaves the best, since the 'iminologues' ($R_2\mathrm{N}-\mathrm{C}=\mathrm{N}-\mathrm{C}\equiv\mathrm{N}$) are characterized by the longest nitrile bond lengths [1.153 (3) Å], a mean value of τ closer to 120° [119.8 (1)°], and a mean value of h nearly equal to zero [0.05 (1)]. On the contrary, the phenyl group seems to be the worst transmitter, since the 'benzologues' ($R_2\mathrm{N}-\mathrm{Ph}-\mathrm{C}\equiv\mathrm{N}$) have the shortest nitrile bond lengths [1.146 (1) Å], the lowest mean τ value of the push–pull systems [117.7 (5)°] and the largest value of h [0.19 (3) Å].

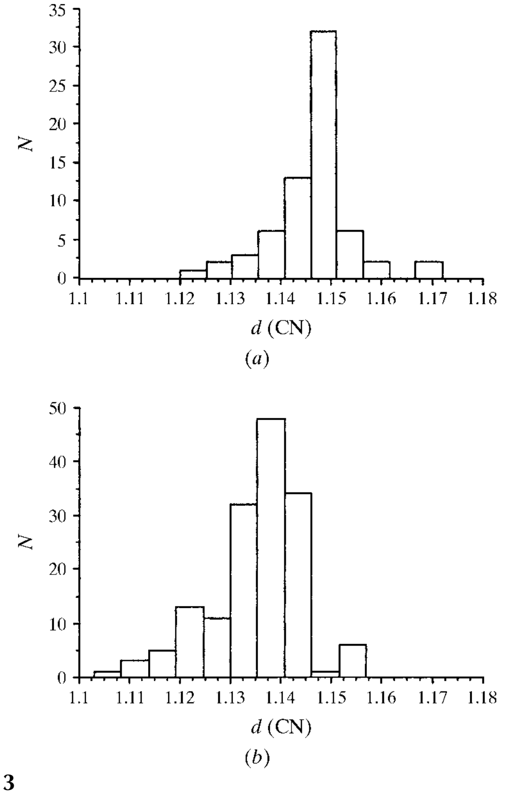

Figure 3
Histogram of the $d(\mathrm{C}\equiv\mathrm{N})$ bond lengths in systems (*a*) (II*b*) and (*b*) (III).

The relative structural features of amino and cyano N atoms in push–pull and aliphatic aminonitriles should be associated with a specific behaviour towards HB donors. In push–pull nitriles, the amino nitrogen lone pair should not be available for HB interactions, whereas in these systems the HB ability of the cyano nitrogen should be reinforced by the resonance effects. Conversely, in aliphatic nitriles the amino nitrogen should use its HB ability, the cyano nitrogen becoming a less appealing candidate. To check the validity of this behaviour, we have analysed the HB contacts observed in the CSD for systems (I), (II) and (III).

3.1.2. Intermolecular hydrogen bonding to amino and cyano N atoms in push–pull and aliphatic nitriles. In this section we analyse the HB contacts observed in the CSD on the amino and cyano nitrogen in systems (I), (II*a*)–(*c*) (push–pull nitriles) and (III) (aliphatic nitriles) by examining

(i) the frequency of contacts on the two HBA;

(ii) the HB geometrical descriptors of the various interactions.

Table 2 presents the number of HB observed on the amino and cyano N atoms in the structures found in the CSD for the different systems. The number of entries in which both HBA are engaged in HB is also reported. In all the competitive examples, we found no or very few HB on the amino nitrogen. Virtually all HB were formed on the cyano nitrogen. A crude estimate of the relative propensity of these two HBA to interact with HB donors can be obtained by the ratio $N_{\mathrm{HB}}/N_{\mathrm{obs}}$, where N_{HB} is the number of HB and N_{obs} is the number of fragments found in the various refcodes [one fragment being one example of the system under investigation (I)–(III) with one HX HB donor]. This ratio varies from *ca* 37% (II*c*) to 87% (II*a*) for the cyano nitrogen in push–pull nitriles, whereas we found no structures in which *only the amino nitrogen* is involved in an HB. In fact, in systems (II*b*) and (II*c*), three and one HB are respectively observed on this atom, the cyano nitrogen also being involved in HB interactions. Conversely, we were surprised to find a very low number of contacts on the amino nitrogen in system (III), since the amino lone pair should still be available for HB interactions. Furthermore, crude benchmarks of $\mathrm{p}K_{\mathrm{HB}}$ for N atoms in aliphatic amines and nitriles are indeed in favour of the amino nitrogen since, with comparable hydrocarbon substituents, these values are 2.10 and 0.90, respectively (Laurence & Berthelot, 2000). A careful examination of the statistics of Table 2 for this group reveals interesting characteristics:

(i) the frequency of contacts on the cyano nitrogen is *ca* 20%, *i.e.* significantly less than that estimated in push–pull nitriles;

(ii) four HB are observed *only on the amino nitrogen* in this system.

Table 2
Number of HB observed in the CSD on the amino and nitrile fragments of the various systems investigated in the present work.

$N_{\rm ent}$ refers to the number of refcodes containing the various fragments and HB donors (HX, X = N, O); $N_{\rm obs}$ is the number of observations. Fragment entries (observations) in which N amino (N nitrile)···H$X \leq 2.65$ Å (see §2).

System	$N_{\rm ent}$ ($N_{\rm obs}$)	Fragments with HB to N amino	Fragments with HB to N nitrile	Fragments with HB to both N
(I)	6 (9)	0	3 (4)	0
(II*a*)	10 (15)	0	10 (13)	0
(II*b*)	92 (250)	3 (3)	70 (100)	3 (3)
(II*c*)	28 (93)	1 (1)	28 (35)	1 (1)
III†	45 (81)	5 (5)	13 (15)	1 (1)

† For n = 1, 2, 3 and 4 (see text).

These observations confirm the loss of the amino nitrogen HB ability to the benefit of the cyano nitrogen in push–pull nitriles because of the conjugative interactions between the amino nitrogen lone pair and the nitrile nitrogen through the π system of the transmitter. In the absence of resonance effects between the two functions, the cyano nitrogen becomes a weaker HB acceptor compared with push–pull nitriles, the amino nitrogen again becoming able to use its HB accepting potential. The weak number of contacts on the amino nitrogen in this system can therefore be explained by steric factors that would prevent HB formation. Individual examination of the four structures (GATZOQ, Henkel *et al.*, 1997; JAPHOX, Foresti *et al.*, 1989; PAZJAB, Vilsmaier *et al.*, 1996; RILBET, Kozikowski *et al.*, 1997), in which HB are formed on the amino nitrogen, is in agreement with this influence since in three of them the amino nitrogen belongs to six-membered (JAPHOX, RILBET) or five-membered cycles (PAZJAB) in which the nitrogen lone pair is particularly uncrowded. The value of τ in the three structures, 110.4, 110.3 and 109.0, respectively, confirms this lack of steric hindrance since it is significantly lower than the mean value of 112.0 (4)° obtained for aliphatic aminonitriles (Table 1). This feature is illustrated in Fig. 4, which shows the histogram of the τ valence angles in system (III) with the positions of the τ values of JAPHOX, PAZJAB and RILBET indicated.

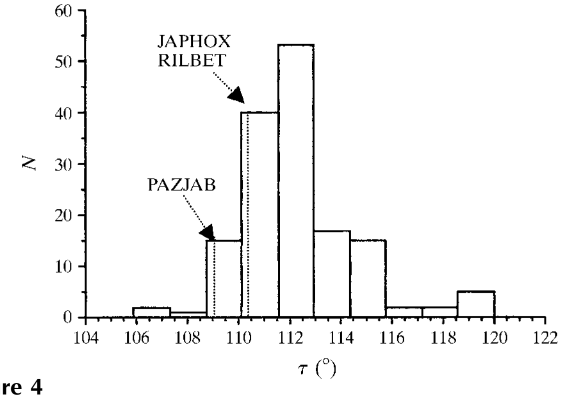

Figure 4
Histogram of the τ valence angles in system (III) (aliphatic nitriles). The position of the values observed for the structures in which the amino nitrogen is involved in hydrogen-bonding interactions is represented by a vertical line.

Table 3
Geometric parameters of the HB observed in the CSD for structures in which both amino and cyano N atoms are HB acceptors.

N_1: amino nitrogen atom; N_2: nitrile nitrogen atom.

Refcode		AMFURB		DAMALN		DAMALN01	
system	N_1	N_2	N_1	N_2	N_1	N_2	
(II*b*)	d(H···N) (Å)	2.29	2.08	2.18	2.18	2.18	2.16
	d(N···X)† (Å)	3.27	3.01	3.27	3.13	3.15	3.11
	α(NH···X)† (°)	164.6	151.2	164.4	154.6	160.9	156.3
	θ(CN···H) (°)	97.8	167.2	108.7	144.2	110.3	171.4
	d(C≡N)		1.137		1.136		1.134

		CYAMPD03	
		N_1	N_2
(II*c*)	d(H···N) (Å)	2.65	2.08
	d(N···X)† (Å)	3.34	3.00
	α(NH···X)† (°)	125.8	124.8
	θ(CN···H) (°)	89.9	150.1
	d(C≡N)		1.170

		CPRPCY	
		N_1	N_2
(III)	d(H···N) (Å)	1.89	2.15
	d(N···X)† (Å)	2.84	3.13
	α(NH···X)† (°)	162.4	175.6
	θ(CN···H) (°)	109.1	128.1
	d(C≡N)		1.139

† X: N or O atom of the HB donor.

To obtain further evidence on the relative HB properties of amino and cyano nitrogen in systems (I), (II*a*)–(*c*) and (III), we have analysed the HB experimental geometric features obtained from the CSD.

Table 3 compares the geometric parameters (see §2) of the HB involving both amino and cyano N atoms for push–pull and aliphatic nitriles. As the cyano nitrogen is often involved as a bi- or trifurcated acceptor, only the shortest interaction has been considered in this comparison. The HB abilities of amino and cyano N atoms can be safely compared in the various refcodes of Table 3 since they involve the same HB donor. For push–pull nitriles, no significant trend relative to the HB abilities of the amino and nitrile acceptors is revealed by these data owing to the low number of structures. However, a careful examination of CYAMPD03 (2-cyanoguanidine; Hirshfeld & Hope, 1980), which belongs to the iminologues (II*c*), reveals interesting features. In this structure (Fig. 5), the HB involving the —NH$_2$ donor is significantly shorter on the nitrile nitrogen (2.08 Å) than on the amino nitrogen (2.65 Å). These HB parameters are in agreement with the increased HB ability of the cyano nitrogen through imino formation (Berthelot, Helbert, Laurence, Le Questel, Anvia & Taft, 1993) and the decreased HB ability of an —NH$_2$ amino nitrogen carried by an unsaturated substituent. The last example of Table 3, CPRPCY (Humblet *et al.*, 1977), representative of the aliphatic aminonitriles (III), also reveals interesting features. In contrast to the push–pull nitriles of Table 3, the d(Nsp^3···H) distance is significantly shorter

(1.89 Å) than the $d(Nsp\cdots H)$ distance (2.15 Å; Fig. 6). This stronger HB ability of the amino nitrogen is consistent with the greater HB basicity of tertiary amines relative to aliphatic nitriles, as observed in the pK_{HB} for N atoms in aliphatic amines and nitriles with comparable hydrocarbon substituents (Laurence & Berthelot, 2000).

The α (NH$\cdots X$) angles observed on the amino and cyano nitrogen, relative to the linearity of the HB interactions, range from 125.8 to 164.6 ° and from 124.8 to 175.6 °, respectively, with mean values of 155.6 and 152.6 ° (Table 3). The low number of data in this data set does not allow any relationship to be seen between the HB lengths and the α angles. The θ(CN$\cdots$H) angles can be used to study the directionality of the HB involving the amino and cyano N atoms. These values range from 97.8 to 110.3° and from 128.1 to 171.4°, respectively, with averages of 103.2 and 152.2°. They are in agreement with the direction of a putative lone pair for the sp^3 amino nitrogen and a preference for values close to 150° for the sp nitrile nitrogen (Le Questel *et al.*, 2000).

To confirm the influence of the transmitting group separating the amino and nitrile functions on the cyano nitrogen HB ability, we have analysed the geometric parameters of the HB formed on this atom in systems (I), (II*a*)–(*c*) (push–pull nitriles) and (III) (aliphatic nitriles). These data are gathered in Table 4. If we omit the benzologues (II*a*), all the HB involving the nitrile nitrogen are significantly shorter in push–pull systems than in aliphatic nitriles. Such enhancement of the nitrile nitrogen HB basicity in push–pull nitriles can be attributed to resonance-assisted hydrogen bonding (RAHB) originally pointed out in the solid state by Gilli and coworkers (Gilli *et al.*, 1989) for strong homonuclear hydrogen bonds (*e.g.* O—H$\cdots$O and N—H$\cdots$N) and extended to heteronuclear systems (*e.g.* N—H$\cdots$O), for example, in heterodienic compounds in which N—H$\cdots$O intermolecular HB are assisted by resonance (Gilli *et al.*, 1994, 1996; Bertolasi *et al.*, 1999). It is worth noticing that within the push–pull family, the shortening (strengthening) of the HB on the nitrile nitrogen follows the experimental order of HB basicity as observed in solution through the pK_{HB} scale for comparable systems (Berthelot, Helbert, Laurence, Le Questel, Anvia & Taft, 1993).

	T: Ph (IIa)	<	T: C=C (IIb)	<	T: C=N (IIc)
	Benzologues		Vinylogues		Iminologues
$d(N\cdots H)$ Å	2.22 (2)	<	2.15(2)	<	2.06 (2)
$d(N\cdots X)$ Å	3.14 (2)	<	3.06(1)	<	2.99 (2)
pK_{HB}	1.23	<	1.70	<	2.09
Compound:	Me_2N-Ph-C≡N		Me_2N-CH=CH-C≡N		Me_2N-CH=N-C≡N

The position of cyanamides (I) cannot be defined in this sequence owing to the low number of contacts for this data set. This sequence is consistent with the order of lengthening of the C≡N bond noted in the analysis of the geometrical parameters of the push–pull nitriles, the benzologues being characterized by the shortest C≡N bond lengths and the iminologues by the longest (*see below*). No relation is found between the HB lengths and the α angles of Table 4 since these values are close to 150° for all systems. The directionality angles θ are close to 140°, typical of values already reported for HB interactions on nitriles (Le Questel *et al.*, 2000; Thallapally & Desiraju, 2000). If the cone correction is applied (Kroon *et al.*, 1975), both θ and α angles tend towards a linear geometry.

3.2. Molecular orbital calculations

In order to investigate theoretical descriptors of hydrogen bonding *in vacuo*, we have carried out *ab initio* calculations at the B3LYP/6-31+G** level on model compounds. A reliable description of the structural and energetic properties of hydrogen-bonded systems requires high-level *ab initio* molecular orbital calculations. However, simple analyses based on molecular electrostatic potentials have proved to give excellent predictions of HB basicity (Kenny, 1994). In recent studies, we have used this quantum mechanical descriptor to predict the HB basicity of aliphatic primary amines (Graton *et al.*, 1999) and nitriles (Le Questel *et al.*, 2000). In the present work we have extended this approach to investigate the *relative* HB abilities of cyano and amino N atoms in five model compounds corresponding to the molecular fragments investigated using the CSD. Table 5 shows the various electrostatic

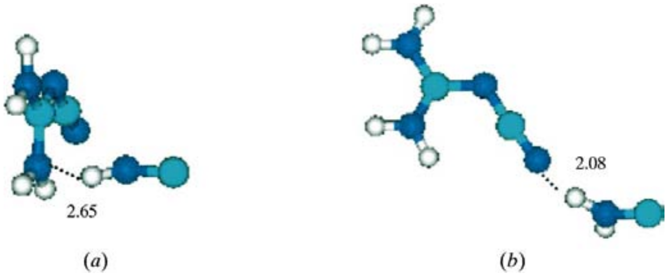

Figure 5
Hydrogen bonds on (*a*) the amino and (*b*) the nitrile N atoms in CYAMPD03 (2-cyanoguanidine).

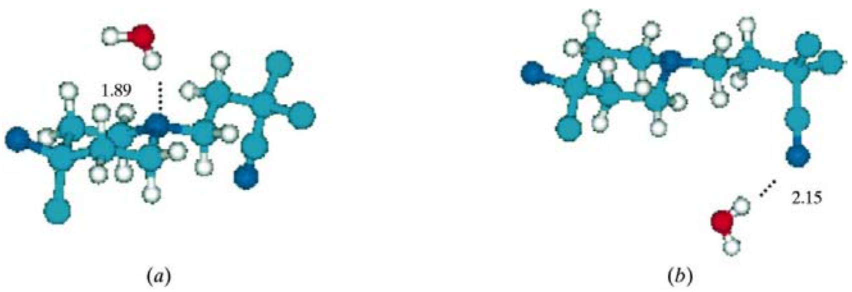

Figure 6
Hydrogen bonds on (*a*) the amino and (*b*) the nitrile N atoms in CPRPCY [1′-(3-cyano-3,3-diphenylpropyl)-1,4′-bipiperidine-4′-carboxamide dihydrate piritramide].

Table 4
Geometric parameters of the HB observed in the CSD on the cyano nitrogen of systems (I), (II*a*)–(*c*) and (III).

N_{ent} refers to the number of refcodes containing the various fragments and HB donors ((N/O)H); N_{obs} is the number of observations; X = O or N atom of the HB donor

System	N_{ent} N_{obs}	$d(N\cdots H)$ (Å)	$d(N\cdots X)$ (Å)	$\theta_1(CN\cdots H)$ (°)	$\alpha_1(NH\cdots X)$ (°)
(I)	3 (4)	2.0 (1)	2.99 (8)	148 (8)	153 (15)
(II*a*)	10 (13)	2.22 (2)	3.14 (2)	137 (3)	152 (3)
(II*b*)	71 (99)	2.15 (2)	3.06 (1)	144 (2)	150 (2)
(II*c*)	29 (34)	2.06 (2)	2.99 (2)	139 (3)	154 (2)
(III)	13 (15)	2.29 (5)	3.16 (3)	134 (3)	149 (5)

Table 5
Electrostatic potentials V (kJ mol^{-1}) calculated at the B3LYP/6-31+G** level for the push–pull (1), (2), (3) and (4) and aliphatic aminonitrile (5) models selected.

The experimental pK_{HB} values of these compounds are also indicated. $-V_s$: value calculated on the molecular surface around the amino nitrogen; $\Delta V_s = |V_{s,min}| - |V_s|$.

No.	Compound	$-V_{s,min}$	$-V_s$	ΔV_s	pK_{HB}
(1)	$Me_2N-C\equiv N$	204.2	72.8	131.4	1.56
(2)	$Me_2N-Ph-C\equiv N$	184.1	30.7	153.4	1.25
(3)	$Me_2N-CH=CH-C\equiv N$	221.3	29.0	192.3	1.70
(4)	$Me_2N-CH=N-C\equiv N$	209.2	†	>209.2	2.09
(5)	$Me_2N-(CH_2)_2-C\equiv N$	44.1	30.1	14	0.92 (N nitrile) 1.16 (N amino)

† Positive.

potential values calculated for these models together with their experimental pK_{HB} values, when available. The nitriles (1)–(4) of Table 5 have been selected as models of the push–pull systems (I) and (II*a*)–(*c*), the 3-dimethylaminopropionitrile (5) being the representative of aliphatic nitriles (III). Despite the use of simple model compounds and of a single theoretical descriptor, the results of Table 5 are generally in good agreement with the crystallographic observations that are obtained from a wide range of chemical environments, and with the pK_{HB} measurements. Thus, in push–pull aminonitriles the most negative value of the electrostatic potential is always found on the cyano nitrogen. Furthermore, the progression of this property follows almost exactly the experimental order of HB basicity, as observed through the pK_{HB} scale and the HB parameters measured in the CSD. Only the value of $V_{s,min}$ calculated for the iminologue is not in agreement with the experimental trends in solution and in the solid state since it is not the most negative of the push–pull systems. The ΔV_s values (Table 5) calculated between the amino and cyano N atoms show a distinct behaviour of push–pull nitriles compared with aliphatic nitriles, in agreement with the experimental data since these values range from *ca* 125.5 to 209.3 kJ mol^{-1} for push–pull nitriles, whereas we calculate a difference of only 58.6 kJ mol^{-1} between the two acceptors in the case of 3-dimethylaminopropionitrile (5). The relative progression of the electostatic potential on the two N atoms is consistent with the experimental data since when ΔV_s is small, our FTIR measurements in dilute solution on these systems confirm unambiguously the formation of two 1:1 hydrogen-bonded complexes on the two N atoms (Graton *et al.*, unpublished). Furthermore, it distinguishes clearly the respective behaviours of push–pull and aliphatic nitriles and constitutes a very good descriptor of HB ability in the nitrile family.

The angular locations of the electrostatic potential minima $V_{s,min}$ have proven their use for the analyses of the directional preferences observed in intermolecular interactions (Brinck *et al.*, 1992). To investigate the respective directional preferences of HB interactions on amino and cyano N atoms, we have calculated the $Csp^3-N_{amino}\cdots V_{s,min}$ and $C\equiv N\cdots V_{s,\,min}$ angles and compared these values to the $Csp^3-N_{amino}\cdots H$ and $C\equiv N\cdots H$ angles measured in the CSD. Table 6 reports these data for the various molecular fragments and their respective models. These data show that *in vacuo* the minimum value of the electrostatic potential is always in the direction of the putative nitrile *sp* nitrogen lone pair, the deviation towards linearity becoming significant for the benzologue (2) (166°). These results support the crystallographic data since, in crystalline environments, such linear arrangements can easily be distorted through molecular packing effects.

The directional preference predicted for HB interactions on the amino nitrogen through the computed $Csp^3-N_{amino}-V_s$ angles is in good agreement with the crystallographic $Csp^3-N_{amino}\cdots H$ angles since the theoretical and experimental angles are close to 105°, showing that HB interactions occur in the direction of the amino nitrogen lone pair. The electrostatic potential isosurface computed at −230.1 kJ mol^{-1} (Fig. 7) for the dimethylaminopropionitrile (5) shows an interesting difference between the two N atoms that could partially explain the better accordance between the computed and observed angles for the amino N atoms than for the cyano N atoms. While the lone pair is strikingly well resolved around the amino nitrogen, a much larger zone of electron density is clearly seen around the cyano nitrogen. In other words, more space appears available for approaching HB donors around the *sp* nitrogen, a tendency in agreement with the greater number of contacts observed on this atom, the wider range of

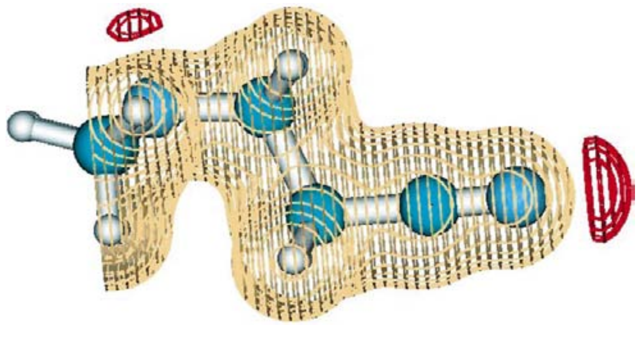

Figure 7
Molecular electrostatic isopotential surface for dimethylaminopropionitrile (5) with $|V|$ = 230.1 kJ mol^{-1}, computed at the B3LYP/6-31+G** level. Beige and red isocontours correspond respectively to values of +230.1 and −230.1 kJ mol^{-1}.

Table 6
Angular location (°) of the electrostatic potential minima V_s calculated at the B3LYP/6-31+G** level around the amino and cyano N atoms for the push–pull (1), (2), (3) and (4) and aliphatic aminonitriles (5) models selected together with the crystallographic angles observed for the corresponding molecular fragments.

No.	Compound	$\mathrm{C{\equiv}N\cdots V_{s,min}}$	$\mathrm{C{\equiv}N\cdots H}$	$\mathrm{(C){-}N}sp^3\cdots V_s$	$\mathrm{(C){-}N}sp^3\cdots \mathrm{H}$
(1)	$\mathrm{Me_2N{-}C{\equiv}N}$	175	148.3	94	†
(2)	$\mathrm{Me_2N{-}Ph{-}C{\equiv}N}$	166	136.9	99	†
(3)	$\mathrm{Me_2N{-}CH{=}CH{-}C{\equiv}N}$	176	145.7	88	105.6
(4)	$\mathrm{Me_2N{-}CH{=}N{-}C{\equiv}N}$	177	138.1	–	89.9
(5)	$\mathrm{Me_2N{-}(CH_2)_2{-}C{\equiv}N}$	179	133.0	104	107.0

† No HB observed on the amino nitrogen in the CSD for these systems (*cf.* Table 2).

Table 7
Mean $d(\mathrm{C{\equiv}N})$ bond lengths (Å) observed in the CSD for the molecular fragments (I)–(III), together with the optimized (B3LYP/6-31+G** level) values calculated for the corresponding models.

System	No.	Model B3LYP/6-31+G**	Observed
(I)	(1)	1.170	1.140 (7)
(II*a*)	(2)	1.166	1.146 (1)
(II*b*)	(3)	1.168	1.148 (2)
(II*c*)	(4)	1.171	1.151 (1)
(III)	(5)	1.162	1.138 (1)

the $\mathrm{C{\equiv}N\cdots H}$ angles (mean value 140°) measured in the CSD and the occurrence of multidentate HB.

Lastly, the resonance effects are well reflected by the optimized nitrile bond lengths reported in Table 7, which compares the computed and observed $d(\mathrm{C{\equiv}N})$ values for the various molecular fragments investigated and their models. The computed bond lengths are consistently too long, the mean absolute error being 0.023 Å. Their relative progression, however, follows the crystallographic trends: the pure $d(\mathrm{C{\equiv}N})$ triple bond length in (5) (1.162 Å) increases in all the push–pull nitriles, the shortest being calculated for the benzologue model (2) (1.166 Å) and the longest for the iminologue (4) (1.171 Å).

4. Conclusions

In the present work we have shown, using crystallographic pK_{HB}: thermodynamic and *ab initio* results, that in $\mathrm{N}{-}T{-}\mathrm{C{\equiv}N}$ and $\mathrm{N{-}(C}sp^3)_n{-}\mathrm{C{\equiv}N}$ molecular systems, the preferred HB acceptor is almost always the nitrile nitrogen. In push–pull nitriles, the amino nitrogen lone pair is not available for HB interactions owing to its delocalization towards the nitrile function through the π system of the transmitter. Among the various transmitter groups T able to transmit resonance effects, the crystallographic data show that an aromatic ring (benzologue) is the least efficient whereas a $\mathrm{{-}C{=}N{-}}$ double bond is the best. These crystallographic trends follow the experimental order of HB basicity measured in solution through the pK_{HB} scale. In aliphatic aminonitriles, both N atoms can act as HB acceptors, but the greater sensitivity of the amino nitrogen to steric crowding leads to a surprisingly low number of contacts.

Despite the use of simple models, the relative progression of the molecular electrostatic potentials calculated at the B3LYP/6-31+G** level is in good agreement with the experimental data. In push–pull nitriles the most negative value of the electrostatic potential on the molecular surface $V_{s,\mathrm{min}}$ always corresponds to the nitrile nitrogen, the difference computed between the two heteroatoms ranging from 125.5 to 209.2 kJ mol^{-1}. Conversely, in aliphatic aminonitriles, this difference becomes only 58.6 kJ mol^{-1}. The angular locations of the $V_{s,\mathrm{min}}$ calculated in the present work are in good agreement with the directional preferences observed in crystalline environments, the greater accordance observed between the theoretical and crystallographic data for the amino nitrogen compared with the cyano nitrogen being explained by the larger zone of electronic density available around the *sp* nitrogen.

Overall, this study shows that the combined use of crystallographic, thermodynamic and theoretical data can provide structural and energetic parameters that enable the HB behaviour of HB acceptors in various chemical environments to be rationalized.

The authors gratefully acknowledge the IDRIS (Institut du Développement et des Ressources en Informatique Scientifique) and the CINES (Centre Informatique National de l'Enseignement Supérieur) for a grant of computational time.

References

Aakeröy, C. B. (1997). *Acta Cryst.* B**53**, 569–586.
Allen, F. H., Baalham, C. A., Lommerse, J. P. M., Raithby, P. R. & Sparr, E. (1997). *Acta Cryst.* B**53**, 1017–1024.
Allen, F. H., Bird, C. M., Rowland, R. S. & Raithby, P. R. (1997). *Acta Cryst.* B**53**, 680–695.
Allen, F. H., Davies, J. E., Galloy, J. J., Johnson, O., Kennard, O., Macrae, C. F., Mitchell, E. M., Mitchell, G. F., Smith, J. M. & Watson, D. G. (1991). *J. Chem. Inf. Comput. Sci.* **31**, 187–204.
Allen, F. H., Kennard, O., Taylor, R., Watson, D. G., Orpen, A. G. & Brammer, L. (1987). *J. Chem. Soc. Perkin Trans. 2*, pp. S1–S19.
Alkorta, I., Rozas, I. & Elguero, J. (1998). *Theor. Chem. Acc.* **99**, 116–123.
Berthelot, M., Helbert, M., Laurence, C. & Le Questel, J.-Y. (1993). *J. Phys. Org. Chem.* **6**, 302–306.
Berthelot, M., Helbert, M., Laurence, C., Le Questel, J.-Y., Anvia, F. & Taft, R. W. (1993). *J. Chem. Soc. Perkin Trans. 2*, pp. 625–627.
Bertolasi, V., Gilli, P., Ferretti, V., Gilli, G., Vaughan, K. & Jollimore, J. V. (1999). *Acta Cryst.* B**55**, 994–1004.
Besseau, F., Laurence, C. & Berthelot, M. (1994). *J. Chem. Soc. Perkin Trans. 2*, pp. 485–489.
Besseau, F., Laurence, C. & Berthelot, M. (1996). *Bull. Soc. Chim. Fr.* **133**, 381–387.
Böhm, H.-J., Brode, S., Hesse, U. & Klebe, G. (1996). *Chem. Eur. J.* **2**, 1509–1513.

Brinck, T., Murray, J. S. & Politzer, P. (1992). *Int. J. Quant. Chem.* **19**, 57–64.

Bruno, I. J., Cole, J. C., Rowland, R. S., Taylor, R. & Verdonk, M. L. (1997). *J. Comput. Aided Mol. Des.* **11**, 525–537.

Cambridge Crystallographic Database (1994). *Quest User's Guide for Vista.* 12 Union Road, Cambridge, England.

Cambridge Crystallographic Database (1995). *Vista User's Guide*. 12 Union Road, Cambridge, England.

Chardin, A., Laurence, C., Berthelot, M. & Morris, D. G. (1996*a*). *J. Chem. Soc. Perkin Trans. 2*, pp. 1047–1051.

Chardin, A., Laurence, C., Berthelot, M. & Morris, D. G. (1996*b*). *Bull. Soc. Chim. Fr.* **133**, 389–393.

Desiraju, G. R. (1997). *Chem. Commun.* pp. 1475–1482.

Etter, M. C. & Reutzel, S. M. (1991). *J. Am. Chem. Soc.* **113**, 2586–2598.

Foresti, E., Sabatino, P., Riva di Sanseverino, L., Tosi, C., Fusco, R. & Tonani, R. (1989). *Acta Cryst.* C**45**, 1039–1044.

Frisch, M. J., Trucks, G. W., Schlegel, H. B., Gill, P. M. W., Johnson, B. G., Robb, M. A., Cheeseman, J. R., Keith, T., Petersson, G. A., Montgomery, J. A., Raghavachari, K., Al-Laham, M. A., Zakrzewski, V. G., Ortiz, J. V., Foresman, J. B., Cioslowski, J., Stefanov, B. B., Nanayakkara, A., Challacombe, M., Peng, C. Y., Ayala, P. Y., Chen, W., Wong, M. W., Andres, J. L., Repogle, E. S., Gomperts, R., Martin, R. L., Fox, D. J., Binkley, J. S., Defrees, D. J., Baker, J., Stewart, J. P., Head-Gordon, M., Gonzales, C. & Pople, J. A. (1995). *Gaussian.* Gaussian, Inc., Pittsburgh PA.

Gilli, G., Belluci, F., Ferretti, V. & Bertolasi, V. (1989). *J. Am. Chem. Soc.* **111**, 1023–1028.

Gilli, P., Bertolasi, V., Ferretti, V. & Gilli, G. (1994). *J. Am. Chem. Soc.* **116**, 909–915.

Gilli, P., Ferretti, V., Bertolasi, V. & Gilli, G. (1996). *Advances in Molecular Structure Research*, edited by M. Hargittai and I. Hargittai, Vol. 2, pp. 67–102. Greenwich, CT: JAI.

Graton, J., Laurence, C. & Berthelot, M. (2001). Unpublished results.

Graton, J., Laurence, C., Berthelot, M., Le Questel, J.-Y., Besseau, F. & Raczynska, E. D. (1999). *J. Chem. Soc. Perkin Trans. 2*, pp. 997–1001.

Gurka, D. & Taft, R. W. (1969). *J. Am. Chem. Soc.* **91**, 4794–4801.

Henkel, S., Meunier, N. & Jager V. (1997). *Z. Kristallogr. New Cryst. Struct.* **212**, 221–222.

Hirshfeld, F. L. & Hope, H. (1980). *Acta Cryst.* B**36**, 406–415.

Humblet, H., Evrard, G. & Durant, F. (1977). *Acta Cryst.* B**33**, 1615–1617.

Jeffrey, G. A. & Saenger, W. (1991). *Hydrogen Bonding in Biological Structures.* Berlin: Springer.

Kenny, P. W. (1994). *J. Chem. Soc. Perkin Trans. 2*, pp. 199–202.

Kozikowski, A. P., Araldi, G. L. & Ball, R. G. (1997). *J. Org. Chem.* **62**, 503–509.

Kroon, J., Kanters, J. A., van Duijneveldt-van der Rijdt, J. G. C. H., van Duijneveldt, F. B. & Vliegenthart, J. A. (1975). *J. Mol. Struct.* **24**, 109–129.

Laurence, C. & Berthelot, M. (2000). *Perspect. Drug Discov. Des.* **18**, 39–60.

Laurence, C., Berthelot, M., Le Questel, J.-Y. & El Ghomari, M. J. (1995). *J. Chem. Soc. Perkin Trans. 2*, pp. 2075–2079.

Le Questel, J.-Y., Berthelot, M. & Laurence, C. (2000). *J. Phys. Org. Chem.* **13**, 347–358.

Le Questel, J.-Y., Laurence, C., Lachkar, A., Helbert, M. & Berthelot, M. (1992). *J. Chem. Soc. Perkin Trans. 2*, pp. 2091–2094.

Llamas-Saiz, A. L. & Foces-Foces, C. (1992). *Acta Cryst.* B**48**, 700–713.

Lommerse, J. P., Price, S. L. & Taylor, R. (1997). *J. Comput. Chem.* **18**, 757–774.

Nobeli, I., Price, S. L., Lommerse, J. P. M. & Taylor, R. (1997). *J. Comput. Chem.* **18**, 2060–2074.

Rowland, R. S. & Taylor, R. (1996). *J. Phys. Chem.* **100**, 7384–7391.

Schaftenaar, G. & Noordik, J. H. (2000). *J. Comput. Aided Mol. Des.* **14**, 123–134.

Taft, R. W., Gurka, D., Joris, L., Schleyer, P. von R. & Rakshys, J. W. (1969). *J. Am. Chem. Soc.* **91**, 4801–4808.

Thallapally, P. K. & Desiraju, G. R. (2000). *Acta Cryst.* C**56**, 572–573.

Vilsmaier, E., Grosse, M., Schlag, W.-R., Milch, G., Bergstrasser, V. & von Onciul, A. R. (1996). *J. Prakt. Chem.* **338**, 479–484.

Wavefunction, Inc. (1995). *Spartan*4.0. Wavefunction, Inc., 18401 von Karman, No. 210, Irvine, CA, USA.